5-1-2006

Two Fluid Effects On Three-Dimensional Reconnection In The Swarthmore Spheromak Experiment With Comparisons To Space Data

Michael R. Brown
Swarthmore College, doc@swarthmore.edu

C. D. Cothran

Jerome Fung , '06

Two fluid effects on three-dimensional reconnection in the Swarthmore Spheromak Experiment with comparisons to space dataa)

M. R. Brown, C. D. Cothran, and J. Fung

Citation: Physics of Plasmas (1994-present) **13**, 056503 (2006); doi: 10.1063/1.2180729
View online: http://dx.doi.org/10.1063/1.2180729
View Table of Contents: http://scitation.aip.org/content/aip/journal/pop/13/5?ver=pdfcov
Published by the AIP Publishing

Two fluid effects on three-dimensional reconnection in the Swarthmore Spheromak Experiment with comparisons to space data[a)]

M. R. Brown,[b)] C. D. Cothran, and J. Fung
Department of Physics and Astronomy, Center for Magnetic Self Organization, Swarthmore College, Swarthmore, Pennsylvania 19081-1397

(Received 21 October 2005; accepted 14 December 2005; published online 15 May 2006)

Several new experimental results are reported from spheromak merging studies at the Swarthmore Spheromak Experiment [M. R. Brown, Phys. Plasmas **6**, 1717 (1999)] with relevance to three-dimensional (3D) reconnection in laboratory and space plasmas. First, recent velocity measurements of impurity ions using ion Doppler spectroscopy are reported. Bidirectional outflow at nearly the Alfvén speed is clearly observed. Second, experimental measurements of the out-of-plane magnetic field in a reconnection volume showing a quadrupolar structure at the ion inertial scale are discussed. Third, a measurement of in-plane Hall electric field and nonideal terms of the generalized Ohm's law in a reconnection volume of a weakly collisional laboratory plasma is presented. Time resolved vector magnetic field measurements on a 3D lattice $[\mathbf{B}(\mathbf{r},t)]$ enables evaluation of the various terms. Results show that the Hall electric field dominates everywhere $(\mathbf{J}\times\mathbf{B}/ne)$ and also exhibits a quadrupolar structure at the ion inertial scale; resistive and electron inertia terms are small. Each of these is related to and compared with similar measurements in a solar or space context. © *2006 American Institute of Physics*. [DOI: 10.1063/1.2180729]

I. INTRODUCTION

Magnetic reconnection is a process involving local annihilation of magnetic flux and global rearrangement of magnetic field lines. The process of reconnection necessarily results in a loss of magnetic energy with a subsequent increase in energy of ions and electrons in the plasma (flows and heating). In this paper, we discuss three results from the Swarthmore Spheromak Experiment (SSX) reconnection experiment and corresponding related results from spacecraft. First, a direct laboratory measurement of simultaneous bidirectional outflows from a reconnection volume at a substantial fraction of the Alfvén speed is compared with a similar event in the solar chromosphere. Both measurements rely on high resolution Doppler spectroscopy. Second, a laboratory measurement of the "out-of-plane" quadrupolar magnetic structure in the reconnection zone using 600 magnetic probes is compared to a similar structure at the Earth's magnetopause measured by the spacecraft Polar. Third, a laboratory measurement of the "in-plane" Hall electric field is compared to a similar measurement in the Earth's magnetotail measured by the group of spacecraft called Cluster.

Magnetic reconnection has been observed in space in several contexts. In a typical scenario, parcels of magnetized plasma with oppositely directed field lines are convected into a reconnection volume at a relatively slow inflow speed V_{in} and ejected at an outflow speed V_{out} which is often nearly Alfvénic. For example, bidirectional jets emerging from two sides of a reconnection volume have been observed spectroscopically in the solar chromosphere with the ultraviolet spectrometer SUMER (Solar Ultraviolet Measurements of Emitted Radiation instrument) on the satellite SOHO (Solar and Heliospheric Observatory).[1,2] As the oppositely directed field lines convect into the reconnection volume, a current sheet is formed. If the plasma is relatively collisionless (as is often the case in space contexts) then the electron and ion fluids decouple and the current sheet thickness adjusts to about the ion collisionless skin depth (c/ω_{pi}). Different dynamics for electron and ion fluids generate in-plane currents and out-of-plane fields in a characteristic quadrupole structure. Evidence of two fluid effects have been observed both in the magnetopause[3] and the magnetotail.[4]

The SSX is a flexible facility dedicated to the study of magnetic reconnection through the merger of force-free loops of magnetized hydrogen plasma called spheromaks.[5,6] SSX plasmas have electron density up to 10^{21} m^{-3}, temperatures $T_e \sim T_i \cong 20$ eV, and typical magnetic fields of 0.1 T. The plasma is fully ionized and fully magnetized $\rho_i \ll R$, where $R=0.2-0.25$ m is the outer flux conserving boundary of the plasma (defined by a cylindrical copper wall). The Lundquist number S, the ratio of the resistive magnetic diffusion time τ_R to the Alfvén transit time τ_A, is large for SSX, $S \cong 1000$. Accordingly, the global structure of SSX spheromaks is fully in the magnetohydrodynamic (MHD) regime $(S \gg 1, \rho_i \ll R)$.

Previously, we have measured the three-dimensional (3D) structure of magnetic reconnection,[7] the production of beams of energetic ions accelerated by reconnection electric fields,[8] and various terms in the generalized Ohm's law within the reconnecting volume.[9] The scale of the reconnection current sheet in SSX is about $c/\omega_{pi} \cong 2$ cm[10] and Hall effects are large[9] leading us to believe two fluid effects are important. Local 3D structures have been studied with a high resolution magnetic probe array capable of measuring vector

[a)]Paper BI1 3, Bull. Am. Phys. Soc. **50**, 20 (2005).
[b)]Invited speaker. Electronic mail: doc@swarthmore.edu

B on a $5\times5\times8$ grid, 200 simultaneous measurements of vector **B**, at a spatial resolution of about the ion scale (15 mm radially and 18 mm axially which is $\leqslant c/\omega_{pi}$ in SSX).[11] Large scale magnetic structures have been studied at coarser resolution (25 mm resolution radially) with up to 20 linear arrays threading the machine.[12] Alfvénic outflow has been measured both with electrostatic ion energy analyzers[10] and spectroscopically (see the following). Laboratory measurements have recently been used to interpret spacecraft observations.[13] Hall effects have been recently measured by other groups.[14]

In each of the subsequent sections, we discuss first a recently reported reconnection measurement in a space context followed by a related measurement in SSX. Bidirectional outflow is discussed in Sec. II. The quadrupolar structure of the magnetic field is discussed in Sec. III and the Hall electric field is discussed in Sec. IV. Further discussion and summary is presented in Sec. V.

II. BIDIRECTIONAL OUTFLOW

A characteristic signature of reconnection dynamics is a relatively slow inflow into the reconnection volume and rapid, nearly Alfvénic outflow. The inflow speed is regulated in response to the outflow. The outflow should manifest itself as two oppositely directed jets orthogonal to the inflow direction.

A. SOHO SUMER spacecraft measurement in chromosphere

In a remarkable series of measurements, using the SOHO SUMER ultraviolet spectrometer, Innes *et al.*[1,2] monitored the dynamics of a Si_{IV} line (1393 Å) to determine localized flow and heating during explosive reconnection events in the chromosphere. The SUMER spectrometer had a spatial resolution of about 1 arcsec (~700 km on the solar disk) and a spectral resolution of about 0.044 Å (approximately 10 km/s). The entrance slit corresponded to a very small fraction of the solar surface (10^{-5}) and was typically scanned in steps of about 1 arcsec from east to west across the disk at 5 s exposures and eight positions. Scans at high solar latitude were sensitive to flow across the solar surface (nearly along the line of sight) whereas scans at the center of the disk were sensitive to upflows and downflows. Innes *et al.* observed simultaneous red- and blueshifts of the same line corresponding to bidirectional outflow due to reconnection in the chromosphere.

In Fig. 1, a frame from an event lasting 1890 s at the center of the solar disk from 28 May 1996 is depicted. A broad Si_{IV} line with clear evidence of both red- and blue- "shoulders" is shown on the right-hand side. The shoulders correspond to flows up to 100 km/s and localized to $\leqslant$10 000 km in extent. The dashed line is the average profile of the quiet chromosphere. Spatial scans of the north-south oriented slit show that Doppler shifts can change from red to blue in a few arcseconds (i.e., a few ~1000 km) indicating that the jet structures are very small. The explosive events are short-lived lasting typically 60 s and pervade the surface of the sun (up to 30 000 events at any one time).

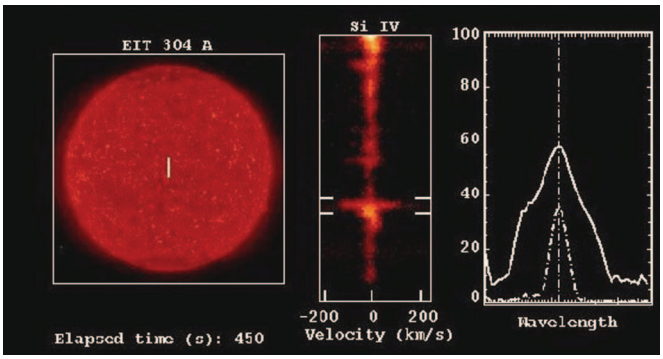

FIG. 1. (Color) Bidirectional flow in the chromosphere. (a) Extreme Ultraviolet Imaging Telescope (EIT) 304 Å image showing position of SUMER slit, (b) Si_{IV} spectrum along the slit at 460 s, and (c) line shape from the central section of the slit showing both blue- and redshifted shoulders.

In these measurements, flow away from the sun (blueshifts) was observed twice as often as toward the sun (redshifts). This is not surprising for observations at the solar center since downward directed jets will be quickly stopped by the dense chromospheric/photospheric material whereas upward directed jets can freely stream into the corona.

B. SSX laboratory measurement

We have recently implemented an ion Doppler spectroscopy (IDS) diagnostic with both high spectral and temporal resolution.[15] This unique instrument combines an echelle grating Czerny-Turner spectrometer with a multianode photomultiplier tube (32 channels each 1 mm wide) to achieve resolving power of $R=\lambda/\delta\lambda\approx5\times10^4$, and time response better than 1 μs (limited by the luminosity of SSX plasmas), sufficient to capture MHD time scale variations in ion flow and temperature. Light is collected from the plasma along a very narrowly diverging view chord approximately 15 mm in diameter. This instrument has been used to record the time dependence of the 229.687 nm C_{III} impurity emission line during spheromak merging experiments. The IDS diagnostic analyzes the C_{III} line at 25th order with a dispersion of 0.008 nm/mm at the detector. Velocity resolution (obtained by fitting the line shape) depends on both signal strength and thermal Doppler width, but can be as good as a few kilometers per second (a few percent of the Alfvén speed); the width [full width at half-maximum (FWHM)] of the instrument function corresponds to 5 km/s (3.4 eV for C ions).

We generate and merge two loops of magnetized plasma containing oppositely directed magnetic fields in order to produce optimal conditions for magnetic reconnection at the midplane of our machine. The two plasma loops have similar density and are convected at a relatively slow inflow speed V_{in} into a highly evacuated, low magnetic field volume. In Fig. 2(a), we depict a schematic representation of the SSX with two plasma loops about to merge. In Fig. 2(b), we show data from a 3D magnetic probe array (600 individual detectors).[11] The full probe array is sampled every 0.8 μs during an experiment, thus resolving MHD fluctuations. The data depicted are from earlier experiments with a 0.5 m flux

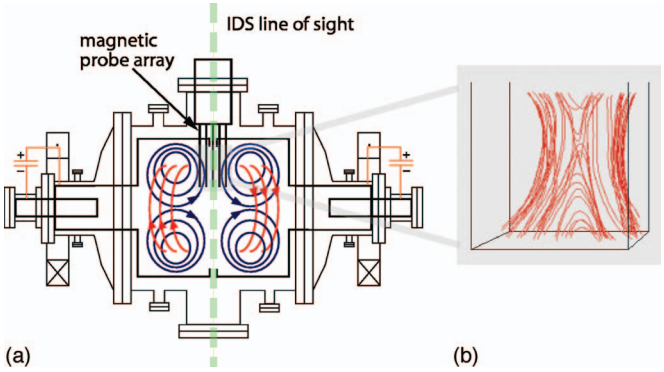

FIG. 2. (Color) Swarthmore Spheromak Experiment. (a) Schematic showing orientation of two merging spheromaks and location of magnetic probe array and (b) magnetic field lines measured by the probe array. Chord for IDS is indicated.

conserver but structure in our new 0.4 m flux conserver is similar. The line of sight for our ion Doppler spectrometer is indicated.

In Fig. 3, we show a sequence of line shapes from C_{III} emission measured during a single reconnection event. The chord for this sequence is across the full 0.4 m diameter at the midplane as shown in Fig. 2. Motion both toward and away from the observer is evident. Simultaneous bidirectional outflow with velocities ±40 km/s is clearly evident in Fig. 3 at about 40 μs.[16] An outflow jet of 40 km/s corresponds to about 0.4 V_A in SSX.

III. QUADRUPOLE MAGNETIC FIELD

In the two fluid model of magnetic reconnection, the ion and electron fluids decouple at the ion inertial scale but the magnetic field remains frozen to the electron fluid. The physical origin of the out-of-plane quadrupole can be understood either by considering the different trajectories of ions and electrons or by considering the dynamics of the electron fluid alone. In the latter argument, the electron fluid flows in a thin layer in the direction opposite the electric current. Since the magnetic field is frozen to the electrons, the electron fluid will tend to drag recently reconnected loops of magnetic field in the electron flow direction. The result is a quadrupolar structure of the magnetic field component in the direction of the electron flow.

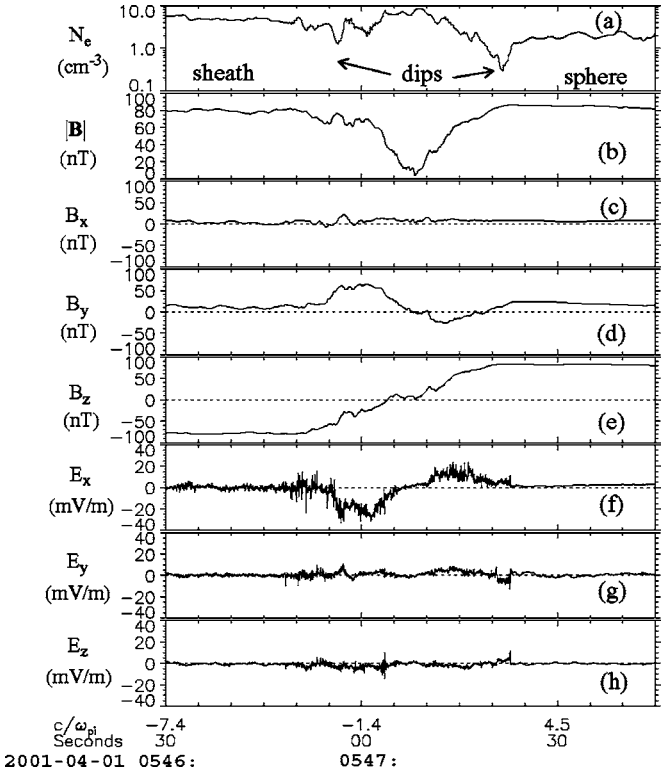

FIG. 4. Polar satellite data at magnetopause. Out-of-plane quadrupole magnetic field is depicted in (d) and the in-plane reconnecting magnetic field in (e). The two lobes of the quadrupole field are about four ion inertial lengths apart.

A. Polar spacecraft measurement in the magnetopause

Recent measurements by the Polar spacecraft at the Earth's magnetopause[3] have shown perhaps the clearest signature of kinetic magnetic reconnection in a single space observation to date. Data from the 28 s 1 April 2001 magnetopause crossing are presented in Fig. 4 with the likely mag-

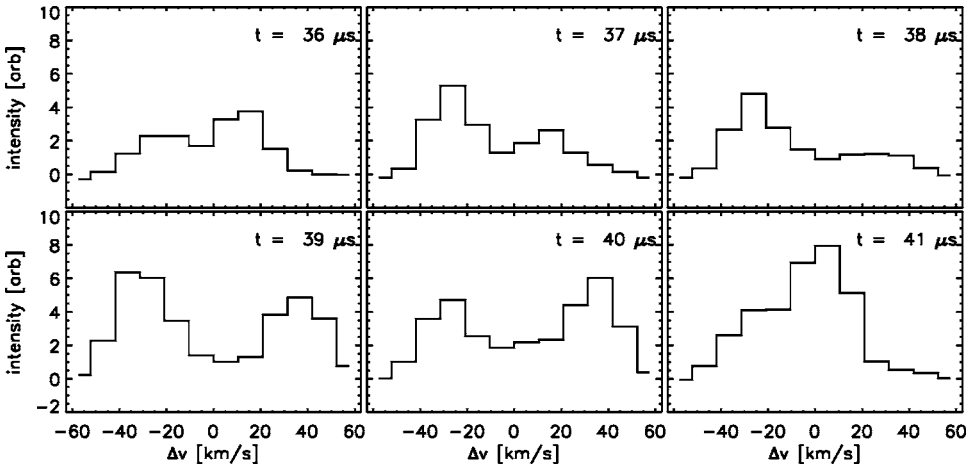

FIG. 3. IDS sequence. Dynamics of C_{III} line are depicted. Bidirectional jets are clearly evident around 40 μs.

netopause geometry in Fig. 5. The geometry of this crossing is fully 3D but the data are rotated and presented in the boundary normal coordinate or minimum variance system to accentuate the two-dimensional (2D) reconnection geometry suggested by theory. It is assumed that the structure does not evolve during the 28 s transit of the reconnection layer. The reconnecting magnetic field clearly reverses sign from southward to northward [Fig. 4(e)], and the out-of-plane magnetic field clearly shows half of the characteristic quadrupole [Fig. 4(d)]. At the magnetopause, the magnitude of the magnetic field nearly vanishes [Fig. 4(b)]. By calculating the magnetopause speed, time can be converted to distance for the single spacecraft. Using the measured plasma density [Fig. 4(a)], distances can be expressed in units of ion inertial scale (c/ω_{pi}). The thickness of the magnetopause measured here is about six magnetosheath ion inertial scales. The two lobes of the quadrupole field are about four ion inertial lengths apart. It is interesting to note that the maximum ion outflow velocity was about 0.4 V_A for this event (similar to the outflow observed in SSX, Sec. II B). Note also that Polar also observed an inward directed electric field correlated with the quadrupole [Fig. 4(f), see Sec. IV].

The direction of the electron flow is opposite the direction of the electric current. For this measurement, the electric current is in the $\hat{\mathbf{y}}$ direction so the electron flow is in the $-\hat{\mathbf{y}}$. If we consider the recently reconnected magnetic field frozen to the electron fluid, the electron flow will tend to pull field lines *into* the page generating the quadrupole pattern. As depicted in Fig. 5, the trajectory of the Polar spacecraft was below the X point, so it observed first a steady negative then positive reconnecting field (B_z) and also, within a few c/ω_{pi} of the X point, a positive going then negative going out-of-plane magnetic field (B_y).

B. SSX laboratory measurement

In Fig. 2, we show a sample of the 3D vector magnetic field (see Cothran *et al.* for details[7]). In order to better compare with space data and theoretical models, we rotate our data to a coordinate system in which the magnetic field most closely resembles a standard 2D X-type reconnection model. This is similar to the boundary normal or minimum variance coordinates of magnetospheric observations. Figure 6 illustrates magnetic data projected onto this plane.[17,18] Note that in SSX this plane is canted relative to the axial direction of spheromak merging due to the twist in each flux tube associated with the toroidal and poloidal field components. Our inflow direction is along $\pm\hat{\mathbf{z}}$. The data shown are from the spontaneous reconnection phase of a counter-helicity merging experiment at time $t=64$ μs.

There is a clear four-lobed quadrupolar structure to the out-of-plane magnetic field, as predicted on theoretical grounds by Sonnerup[19] for collisionless reconnection. To our knowledge, it is the first laboratory measurement of the out of plane magnetic quadrupole. Two lobes of the quadrupole field are aproximately 8 cm or four ion inertial lengths apart. The interpretation is that the measured quadrupolar magnetic field having a magnitude of 100–150 G (up to 25% of the in-plane field) is a consequence of the circulation of the Hall

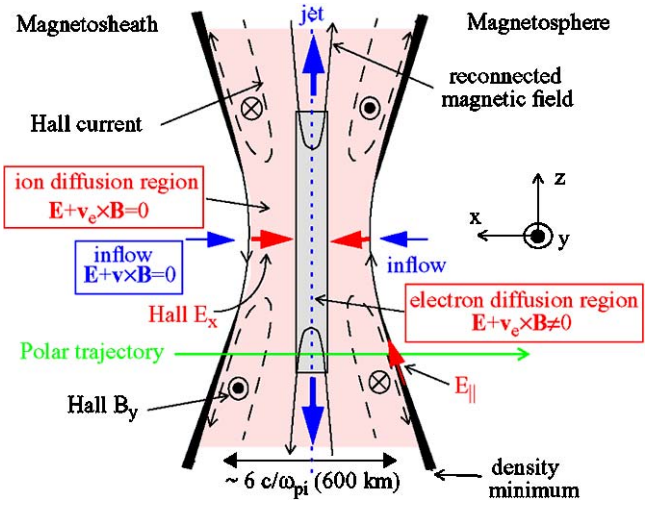

FIG. 5. Geometry of reconnection zone for Polar crossing. Magnetopause inflow direction is $\pm\hat{\mathbf{x}}$.

effect electric field $\mathbf{E}_{\text{Hall}}=\mathbf{J}\times\mathbf{B}/ne$. This term comes into prominence when current sheets thin to $\sim c/\omega_{pi}$, and is a characteristic kinetic signature of reconnection in the low collisionality regime.[19,20]

If a tiny version of the Polar spacecraft traversed our data set, the trajectory would correspond to moving from right to left at $x=-2$ cm. Along this chord, the reconnecting magnetic field is first negative then positive-going while the out-of-plane Hall magnetic field is first positive-going then negative-going (compare Figs. 4 and 5).

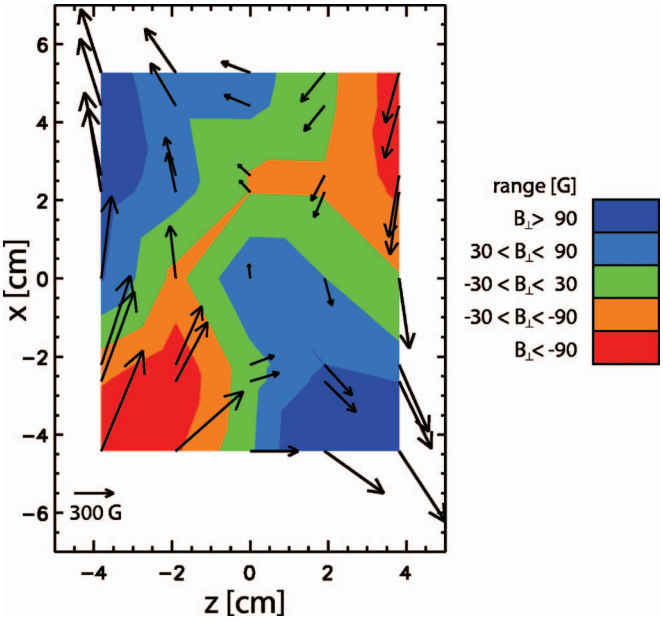

FIG. 6. (Color) SSX quadrupole magnetic field. In-plane reconnecting magnetic field is represented as a vector field. 3D data are projected on a plane that best represents the idealized 2D geometry. SSX inflow direction is the $\pm\hat{\mathbf{z}}$ direction. The scale is indicated with 300 G magnitude vector in the following. Quadrupole field is represented as a color map. Magnitudes reach ±150 G near the outer reaches of the probe array. The ion inertial scale c/ω_{pi} is about 2 cm here. Two lobes of the quadrupole field are about four ion inertial lengths apart.

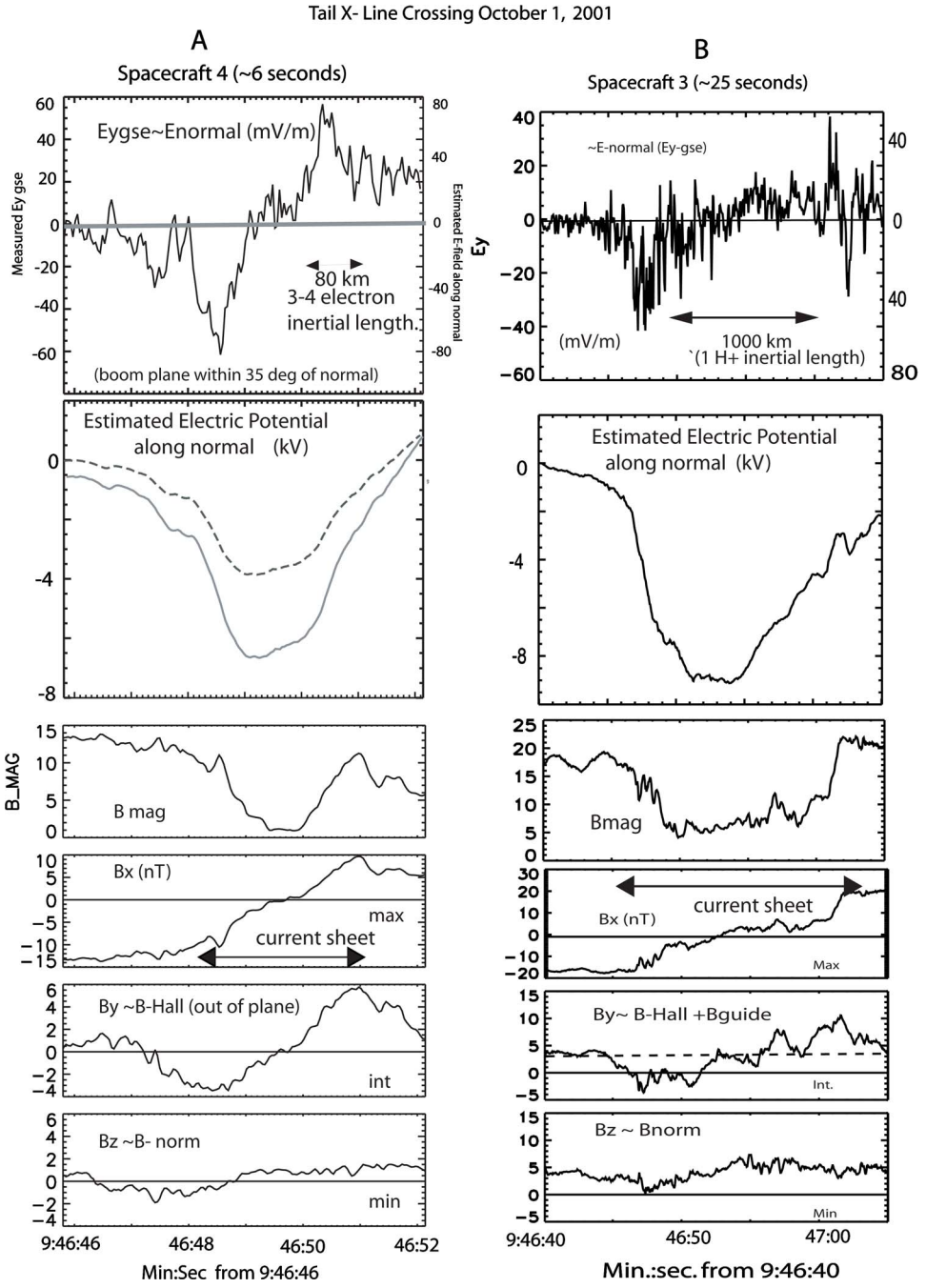

FIG. 7. Cluster satellite data at magnetotail. Column A depicts data from SC-4 near the X line. Column B depicts data from SC-3 approximately 2000 km or two ion inertial scales earthward from SC-4. The in-plane Hall electric field is depicted in the top panel of each column.

IV. HALL ELECTRIC FIELD

In steady state, there will tend to be an inward directed $\mathbf{J}\times\mathbf{B}$ force supporting electron pressure (∇P). If the Hall electric field $\mathbf{J}\times\mathbf{B}/ne$ is the dominant term in the generalized Ohm's law, then E_{Hall} is the dominant part of the total electric field. Large inward directed electric fields have been observed both in space and in the lab.

A. Cluster spacecraft measurement in the magnetotail

Note that reconnection events at the magnetopause discussed in the previous section consist of merging of parcels of magnetofluid from the solar wind and the Earth's magnetosphere. In the magnetopause case, the densities of the merging parcels can be very different and the field lines are not necessarily antialigned. Reconnection in the magnetotail consists of merging of parcels of magnetofluid from the northern and southern lobes with oppositely directed field lines and of similar density. In the magnetotail case, the reconnection geometry is more symmetric than the magnetopause case. Therefore, magnetotail events may have more similarity to SSX merging events.

A careful reader may have noticed that the single spacecraft Polar measured an inward directed electric field at the

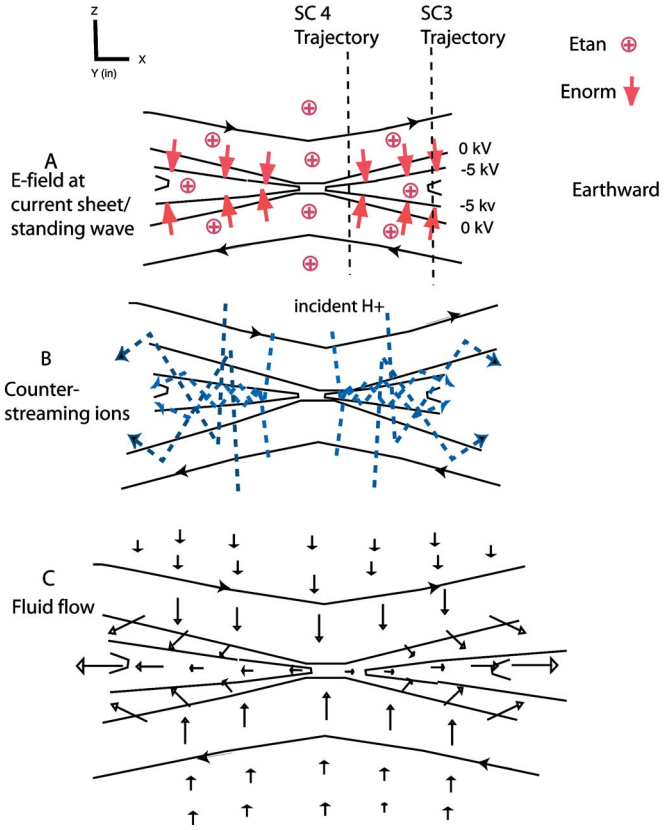

FIG. 8. Geometry of reconnection zone for Cluster crossing. Inward directed electric field, trajectories of ions, and direction of fluid flow are illustrated.

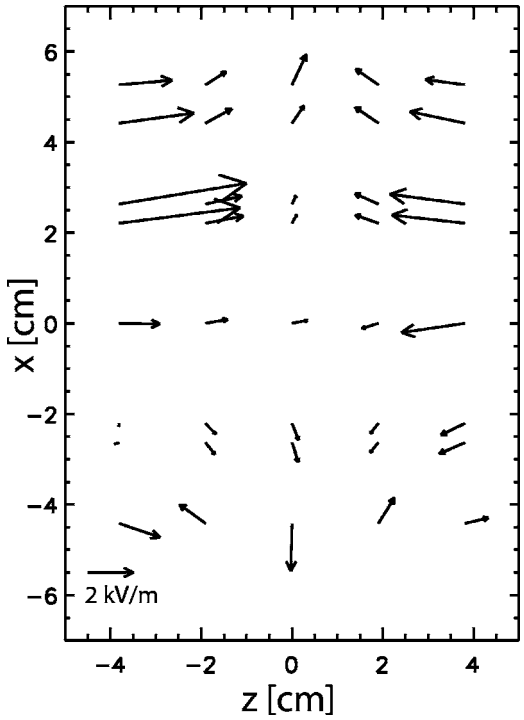

FIG. 9. SSX Hall electric field. A vector map of the projection of the Hall electric field ($\mathbf{J}\times\mathbf{B}/ne$) onto the same plane as depicted in Fig. 6. The Hall electric field is directed inward toward the current sheet and has a quadrupolar character.

magnetopause [Fig. 4(f)]. A more thorough study of the inward directed electric field normal to the current sheet has recently been conducted using the four satellite group called Cluster.[4] The key feature of an ensemble of satellites like the Cluster group is that they are able to distinguish between spatial and temporal features. On 1 October 2001, two of the Cluster spacecraft (spacecrafts 3 and 4, SC3 and SC4) passed through the Earth's magnetotail. Data from the passage of the two satellites are presented in Fig. 7. The left-hand column is the data from SC4 which passed close to the X line. SC3 was closer to Earth (about 2000 km or two ion inertial lengths earthward from SC4) and further from the X line (see Fig. 8). Both spacecraft observed reversal of the reconnecting magnetic field (fourth panel from the top) and both observed the out-of-plane Hall quadrupole magnetic field (fifth panel).

Both also observed an intense inward directed electric field (top panel of each column). However, the spatial scale of the electric field is much different in the two cases. Far from the X line, SC3 observed spatial scales for both the in-plane electric field and the out-of-plane magnetic field at about the ion scale (c/ω_{pi}). This observation is similar to the one made by the Polar spacecraft at the magnetopause and in SSX. SC4 near the X line saw a much sharper spatial scale, just a few electron inertial lengths (c/ω_{pe}).

The direction and rough magnitude of the inward directed electric field can be understood by the following argument. The $\mathbf{J}\times\mathbf{B}$ force (see the following) is directed inward toward the current sheet and acts primarily on the electrons. The ion fluid is coupled to the electron fluid away from the X line but as the plasma flows into the reconnection zone, the ions and electrons decouple with the $\mathbf{J}\times\mathbf{B}$ force tending to drag more electrons than ions into the current sheet. The depth of the potential well is approximately the energy of Alfvénic ions.[4]

B. SSX laboratory measurement

Figure 9 shows a map of the projection of the Hall electric field $\mathbf{J}\times\mathbf{B}/ne$ onto the 2D reconnection plane defined by figure 6 from 3D probe measurements in SSX.[17,18] To our knowledge, it is the first laboratory measurement of the Hall electric field. We use an average electron density in the denominator of the expression. This map is highly similar to the in-plane total electric field shown in Figs. 7 and 8 above from Wygant *et al.*,[4] inferred from Cluster data at a magnetotail tail crossing. Note the important distinction that we measure the Hall electric field magnetically throughout the volume (from $\mathbf{J}$, $\mathbf{B}$, and n) whereas in Cluster it is measured electrostatically along a chord. However, we demonstrate in the following that the Hall contribution dominates the electric field in the generalized Ohm's law in SSX.[9]

The trajectory of the two Cluster spacecraft would correspond to SC4 moving from right to left at $x=+2$ cm and SC3 moving from right to left at $x=+6$ cm. Along these chords, the Hall electric field flips from negative-going to positive-going (compare Figs. 7 and 8). The scale for the

transition for SC3 is about an ion inertial scale while the scale for SC4 (near the X line) was a few electron inertial scales which we cannot resolve in SSX.

The general pattern is essentially that of a flow associated with 2D reconnection: directed inward on the strong field sides of the X point in Fig. 9 ($\pm\hat{\mathbf{z}}$), and outward along the weak field sides (between the interacting spheromaks). This is expected since the Hall electric field is proportional to the Lorentz force, the body force that would drive the expected reconnection flow. Note also that the 2D curl of the vector electric field shown in Fig. 9 is a quadrupolar driver in Faraday's law ($\partial\mathbf{B}/\partial t$). Our measurements support the interpretation that this driving is associated with the out-of-plane Hall magnetic field depicted in Fig. 6.

The Hall electric field mapped in Fig. 9 has a magnitude of several kilovolts per meter at some locations in the SSX reconnection volume. It is useful to compare the magnitude of the Hall electric field to other terms in the generalized Ohm's law.[9] A generalized Ohm's law can be written:

$$\mathbf{E}+\mathbf{u}\times\mathbf{B}=\eta\mathbf{J}+\frac{1}{ne}\mathbf{J}\times\mathbf{B}-\frac{1}{ne}\nabla\cdot\mathbf{P_e}+\frac{m_e}{ne^2}\frac{\partial\mathbf{J}}{\partial t}. \qquad (1)$$

The first term on the right-hand side is the classical collisional resistive dissipation. Next, the Hall term involving $\mathbf{J}\times\mathbf{B}$, associated with differential flow of ions and electrons, becomes appreciable at the ion inertial scale $\rho_{ii}=c/\omega_{pi}$. The electron pressure tensor term is formally of the order of $\beta_e\rho_{ii}$ (where β_e is the ratio of electron pressure to magnetic pressure). The final term in Eq. (1), the electron inertia term, is due to electron dynamics and is appreciable at the electron inertial scale c/ω_{pe}. If the right-hand side vanishes, the "ideal" MHD Ohm's law emerges, $\mathbf{E}+\mathbf{u}\times\mathbf{B}=0$, and, consequently, the magnetic flux is "frozen-in" the bulk plasma moving at the center of mass fluid velocity $\mathbf{u}$.

All three components of the resistive, Hall, and electron inertia electric field terms of the generalized Ohm's law [Eq. (1)] were measured at 200 locations within the reconnection volume (the electron pressure tensor term was not). The time dependence of the magnitude of those terms at one typical point (within c/ω_{pi} of the X line) is shown in Fig. 10. The point corresponds to $(x,z)=(-2,0)$ in Figs. 6 and 9. Data for a single shot are shown in Fig. 10(a) and an ensemble average of 36 shots is shown in Fig. 10(b). The key result is that the Hall term dominates the resistive and electron inertia terms at this and most locations in the reconnection volume and at all times during the discharge. This is so despite the fact that the neutral point is nearby, where the Hall term crosses through zero. The resistive term is 15–70 times weaker than Hall, while the electron inertia is more than four orders of magnitude weaker. Note that we have also measured $\partial\mathbf{B}/\partial t$ and find that the reconnection is evidently occurring quasistatically, in the sense that the overall magnitude $|\partial\mathbf{B}/\partial t|$ is much less than some of the individual terms that contribute to it.

Inspection of Fig. 10 shows that the electron inertial term is negligible, whereas the collisional Ohmic term can support at most about 40 V/m near the neutral point (or line). The Hall term is of the order of 1000 V/m for most of

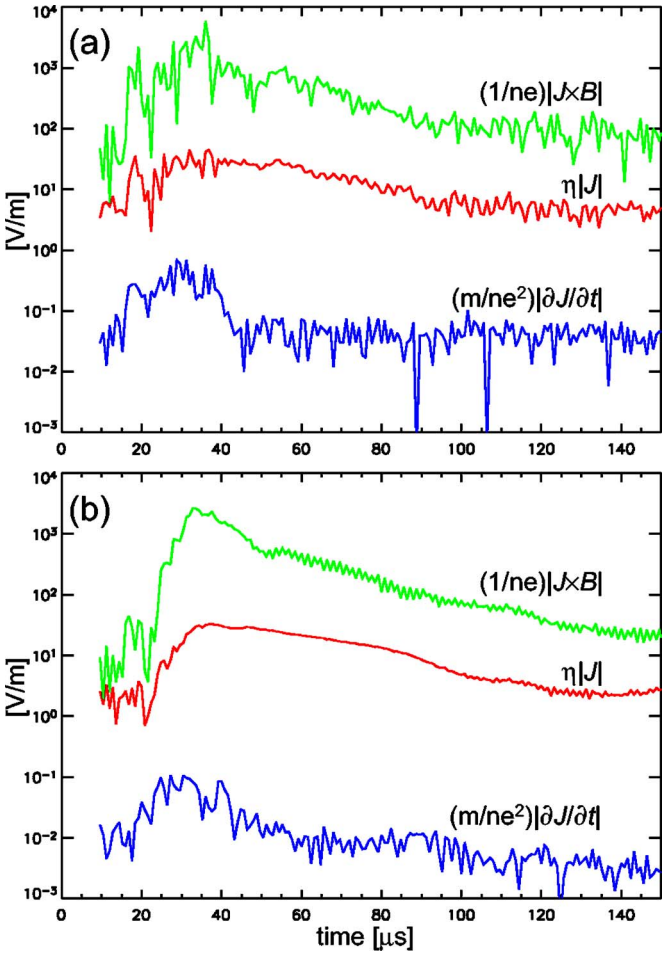

FIG. 10. Time history of resistive, Hall, and electron inertia electric fields from a representative point in the SSX reconnection volume (near the X line). The point corresponds to $(x,z)=(-2,0)$ in Figs. 6 and 9. The Hall term is the dominant contribution to the electric field. Vector magnitudes are presented for simplicity. (a) single shot and (b) ensemble average of 36 shots.

the period from 30 to 70 μs, but cannot contribute at the neutral point, or along a separator. The remaining possibility is that the reconnection electric field at the neutral point is carried by either turbulent resistivity, or by a large electron pressure contribution. Recall now that we have indications that near the SSX reconnection sites there is both quasistatic conditions and near pressure balance. Also, electron and proton temperatures are similar to one another. On this basis, we deduce that $\nabla\cdot\mathbf{P_e}\approx\mathbf{J}\times\mathbf{B}$ in this region. It therefore seems most likely to us that the electric field associated with the electron pressure term carries the reconnection electric field at the neutral point. This inference is subject to the caveat that at the moment we can extract no information experimentally concerning the tensor structure of $\mathbf{P_e}$.

V. SUMMARY

To summarize, several new experimental results are reported from spheromak merging studies at the Swarthmore Spheromak Experiment (SSX) with relevance to 3D reconnection in laboratory and space plasmas. First, we report on recent velocity and temperature measurements of impurity

ions using ion Doppler spectroscopy. Bidirectional outflow at nearly the Alfvén speed is clearly observed. Similar observations have been reported in the solar chromosphere as well as the Earth's magnetosphere. Second, we discuss experimental measurement of the out-of-plane magnetic field near the reconnection zone showing a quadrupolar structure at the ion inertial scale. A similar quadrupolar structure has been observed at the Earth's magnetopause also at the ion inertial scale. Third, we discuss a measurement of in-plane Hall electric field and nonideal terms of the generalized Ohm's law in a reconnection volume of a weakly collisional laboratory plasma. Similar inward directed Hall electric field has been observed in the Earth's magnetosphere (both at the magnetopause and magnetotail).

There are advantages and limitations to experiments in both space and laboratory environments. Space experiments have the advantage of high spatial resolution and essentially nonperturbative measurements. Local measurements of the particle distribution functions are made routinely in space. However, space measurements are typically made only along a one-dimensional trajectory and often temporal and spatial variations are difficult to distinguish. In addition, the global 3D environment is not known and measurements cannot be repeated. Lab experiments have the advantage of full 3D measurements of the spatial structure of dynamical variables. Global structures can measured, temporal and spatial variations are clearly distinguishable, and experiments are repeatable. However, lab experiments generally cannot measure local particle distribution functions (usually only line averages and moments) and generally cannot simultaneously probe the largest and smallest scales (e.g., $R, c/\omega_{pi}, c/\omega_{pe}$). Direct comparisons of measurements of the sort presented previously are important for both the space and laboratory communities. Advantages of one can complement limitations of the other.

ACKNOWLEDGMENTS

This work was performed under the Department of Energy and National Science Foundation. Discussions with D. Innes, F. Mozer, J. Wygant, and S. Cranmer are gratefully acknowledged. Work performed in collaboration with C. Cothran, W. Matthaeus, M. Schaffer, E. Belova, and J. Fung.

[1] D. E. Innes, B. Inhester, W. I. Axford, and K. Wilmelm, Nature (London) **386**, 811 (1997).
[2] D. E. Innes, P. Brekke, D. Germerott, and K. Wilhelm, Solar Physics **175**, 341 (1997).
[3] F. S. Mozer, S. D. Bale, and T. D. Phan, Phys. Rev. Lett. **89**, 015002 (2002).
[4] J. R. Wygant, C. A. Cattell, R. Lysak *et al.*, J. Geophys. Res. **110**, A09206 (2005).
[5] C. G. R. Geddes, T. W. Kornack, and M. R. Brown, Phys. Plasmas **5**, 1027 (1998).
[6] M. R. Brown, Phys. Plasmas **6**, 1717 (1999).
[7] C. D. Cothran, M. Landreman, W. H. Matthaeus, and M. R. Brown, Geophys. Res. Lett. **30**, 1213 (2003).
[8] M. R. Brown, C. D. Cothran, M. Landreman, D. Schlossberg, and W. H. Matthaeus, Astrophys. J. Lett. **577**, L63 (2002).
[9] C. D. Cothran, M. Landreman, M. R. Brown, and W. H. Matthaeus, Geophys. Res. Lett. **32**, L03105 (2005).
[10] T. W. Kornack, P. K. Sollins, and M. R. Brown, Phys. Rev. E **58**, R36 (1998).
[11] M. Landreman, C. D. Cothran, M. R. Brown, M. Kostora, and J. T. Slough, Rev. Sci. Instrum. **74**, 2361 (2003).
[12] C. D. Cothran, A. Falk, A. Fefferman, M. Landreman, M. R. Brown, and M. J. Schaffer, Phys. Plasmas **10**, 1748 (2003).
[13] J. Egedal, M. Oieroset, W. Fox, and R. P. Lin, Phys. Rev. Lett. **94**, 025006 (2005).
[14] Y. Ren, M. Yamada, S. Gerhardt, R. Kulsrud, and A. Kuritsyn, Phys. Rev. Lett. **95**, 055003 (2005).
[15] C. D. Cothran, J. Fung, M. R. Brown, and M. J. Schaffer, "Fast, high resolution Echelle spectroscopy of a laboratory plasma," Rev. Sci. Instrum. (submitted).
[16] C. D. Cothran, J. Fung, M. R. Brown, and M. J. Schaffer, "Simultaneous bi-directional plasma jets from a laboratory magnetic reconnection volume," Phys. Rev. Lett. (submitted).
[17] W. H. Matthaeus, C. D. Cothran, M. Landreman, and M. R. Brown, Geophys. Res. Lett. **32**, L23104 (2005).
[18] M. Landreman, honors thesis, Swarthmore College, Swarthmore, PA (2003).
[19] B. U. O. Sonnerup, *Magnetic Field Reconnection*, in Solar System Plasma Physics, edited by L. T. Lanzerotti, C. F. Kennel, and E. N. Parker (North-Holland, New York, 1979), Chap. III.1.2.
[20] M. A. Shay *et al.*, J. Geophys. Res. **103**, 9165 (1998).